JOURNAL OF SOLID STATE CHEMISTRY 107, 134–148 (1993)

Phases in the System $Ba_2M_{2-x}Cu_xO_{4+\delta}$, M = In, Sc: Structure and Oxygen Stoichiometry

D. H. GREGORY AND M. T. WELLER

Department of Chemistry, The University of Southampton, Southampton, SO9 5NH, United Kingdom

Received October 9, 1992; in revised form March 22, 1993; accepted March 24, 1993

Members of the series $Ba_2M_{2-x}Cu_xO_{4+\delta}$, M = In, Sc ($0 \le x \le 1$), have been synthesised by solid-state reaction methods and products characterized by powder X-ray diffraction (PXD). Selected compounds have been annealed under oxygen at 1 atm and oxygen stoichiometries for unannealed and oxygen annealed samples have been calculated following thermogravimetric analysis (TGA). Structures for M = In, x = 0, 0.5, 1 and M = Sc, x = 1 were determined by Rietveld analysis of PXD data. $Ba_2In_2O_5$ has been shown to crystallize in the orthorhombic space group *Ibm*2 (Brownmillerite structure) with a = 6.0956(1) Å, b = 16.7112(3) Å, c = 5.9601(1) Å. The copper-containing phases adopt a tetragonal "doubled perovskite" structure built up of copper-substituted $BaInO_{2.5}$ cubes. The copper coordination and oxidation state can be controlled by varying the oxygen level of the structure. © 1993 Academic Press, Inc.

Introduction

Many studies of compounds formed in the BaO–In_2O_3 system have been carried out (*1–4*) including single-crystal X-ray diffraction studies which show that many of these compounds are derived from the perovskite structure. $Ba_3In_2O_6$ adopts a tetragonal structure (space group *I4/mmm* a = 4.1868 Å, c = 21.7041 Å) bearing a notable resemblance to $La_2SrCu_2O_6$ (*5*). $Ba_4In_2O_7$ (*I4/mmm* a = 4.175 Å, c = 29.483 Å) (*6*) is also closely related with In^{3+} found in layers of InO_5 square pyramids. The simplest compound in the system, $BaInO_{2.5}$, crystallizes as an oxygen-deficient perovskite forming a cubic structure (a = 4.219(2) Å) (*7*) with In^{3+} in the six-fold B corner site. $Ba_4In_6O_{13}$ adopts an orthorhombic structure (a= 11.899(3) Å, b = 20.567(5) Å, c = 5.975(2) Å) (*8*) with cell parameters related to the $BaInO_{2.5}$ perovskite: $a \approx 2\sqrt{2}a_p$, $b \approx 5a_p$, and $c \approx \sqrt{2}a_p$ (where a_p is the lattice parameter of the perovskite $BaInO_{2.5}$). The indate $Ba_8In_6O_{17}$ is an intergrowth of oxygen-deficient $BaInO_{2.5}$ perovskite blocks and BaO rocksalt layers. The structure is tetragonal (a = 4.1725 Å, c = 30.4870 Å) and the coordination of indium to oxygen is partially lowered to 5 (*9*, *10*). $BaIn_2O_4$, however, is not perovskite related and crystallises with monoclinic symmetry (a = 14.432 Å, b = 5.833 Å, c = 20.792 Å, β = 110.02°) (*11*).

A variety of other indate phases can be obtained by either partially or fully substituting different alkaline earth ions for Ba^{2+}. $CaIn_2O_4$ is orthorhombic with a = 9.65(1) Å, b = 11.30(1) Å, and c = 3.21(1) Å (*1*). $SrIn_2O_4$ is also orthorhombic and crystallises in space group *Pnam* (a = 9.809 Å, b = 11.449 Å, c = 3.265 Å) (*12*). Sr^{2+}can be partially substituted for Ba^{2+} in $Ba_3In_2O_6$ to give $Ba_2SrIn_2O_6$ (*13*) and $BaSr_2In_2O_6$ (*14*); both compounds are isostructural with $Ba_3In_2O_6$, with the cell contracting as Sr^{2+} replaces Ba^{2+}. The calcium analogues $Ca_3In_2O_6$ (*15*) and $SrCa_2In_2O_6$ (*16*), however, crystallize in orthorhombic symmetry (space group *Pbam*). Strontium also forms

0022-4596/93 $5.00

the indate $Sr_2In_2O_5$ which forms the Brownmillerite structure (a = 6.049 Å, b = 15.84 Å, c = 5.81 Å) (*17*).

Studies of the system $BaO–Sc_2O_3$ have shown that phases exist apparently analogous to the indate phases above (*18*). These, however, are not necessarily isostructural. $BaSc_2O_4$ forms a triclinic cell (a = 20.578(7) Å, b = 9.836(3) Å, c = 5.812(2) Å, α = 90.01°, β = 90.01°, γ = 89.88°) (*3*). $Ba_2Sc_2O_5$ has been identified as forming a tetragonal perovskite structure (a = 4.1517 Å, c = 3.9857 Å) (*18*) which is a distorted analogue of $BaInO_{2.5}$. A compound of composition $Ba_3Sc_4O_9$ has also been shown to exist. This crystallizes in hexagonal symmetry (a = 5.78 Å, c = 23.69 Å) (*19*).

More recently Kharlanov *et al.* (*20*) have succeeded in synthesising a number of compounds based on barium–metal oxides (in which the metal can be indium, scandium, or lutetium) in which copper is partially substituted for the trivalent metal cation (M^{3+}). In each case the structure is perovskite based with Ba^{2+} on the A site and the sixfold-coordinated B site occupied by M^{3+} and substituted copper. The reported phases are oxygen deficient as a result of substituting Cu^{2+} for M^{3+}. The phases $Ba_2MCuO_{4.5}$ (M = In, Sc, Lu) and $Ba_3Sc_2CuO_7$ are essentially doubled and tripled Ba MO_{3-x} perovskite blocks in which one M^{3+} has been fully substituted by one Cu^{2+}. The phases $Ba_3M_4Cu_3O_{12}$ (M = In, Sc) and $Ba_4InCuO_{6.5}$ are examples of existing barium–metal oxides in which M^{3+} has been replaced by one or more copper ions. All the phases crystallize in the tetragonal system.

Refinement of powder X-ray diffraction data for $Ba_2ScCuO_{4.5}$ showed the structure to be a tetragonal arrangement of two copper-substituted $BaScO_{2.5}$ cubes in which Sc^{3+} and Cu^{2+} order occupying distinct alternating B positions (Fig. 1). The structure is oxygen-deficient with partial occupation of the oxygen (O_{III}) site at ($\frac{1}{2}$, 0, $\frac{1}{2}$). This partial vacancy leads to an essentially linear coordination for copper with $Cu–O_{II}$ bond lengths of 1.81(9) Å. The $Cu–O_{III}$ bond lengths are much larger at 2.065 Å. The 25% occupancy of O_{III} also leads to a decrease in the Ba^{2+} coordination number from 12 to an average value of 9.

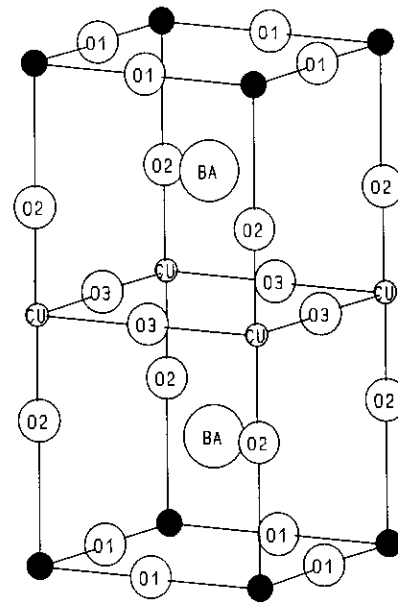

FIG. 1. Structure of $Ba_2ScCuO_{4.5}$; Ba^{2+} site is marked BA, Sc^{3+} site is unmarked and shaded, Cu^{2+} site is marked CU, O^{2-} sites are marked O1, O2, and O3.O3 is only partially (25%) occupied.

This study concerns the synthesis and structure of the simplest copper-substituted phase $Ba_2MCuO_{4+\delta}$ (M = In, Sc) and the solid solution $Ba_2In_{2-x}Cu_xO_{4+\delta}$ ($0 \le x \le 1$). It also examines the effect of oxygen annealing on the structure and copper coordination. The relationship of this structure to superconducting copper oxide structures is discussed.

Experimental

The solid solutions $Ba_2M_{2-x}Cu_xO_{4+\delta}$ (M = In, Sc) were synthesized by high-temperature solid-state reaction of $BaCO_3$ (99.9%), CuO (99.995%), and either In_2O_3 (99.9%) or Sc_2O_3 (99.99%). x = 1 samples for M = In, Sc were fired at 1000°C in air for at least 72 hr with regrindings every

24 hr. For $x < 1$, M = In, higher sintering temperatures were used up to about 1050°C. For the $x = 0$ sample, however, still higher sintering temperatures were needed, typically ~1300°C. Selected samples were oxygen annealed at 1000°C/1 atm O_2 for 24 hr and slow cooled under oxygen.

Powder X-ray diffraction (PXD) data were collected on a Siemens D-5000 Θ–2Θ diffractometer using Cu$K_{\alpha 1}$ radiation. Data were used to check sample purity and to calculate cell parameters by least squares fitting. Full profile refinement data were collected for $x = 0$, 0.5, 1, M = In and $x = 1$, M = Sc samples at slower scan rates, typically over a period of 8–10 hr, in the angular range 10°–90° 2Θ. Data points were collected every 0.02° in 2Θ.

The oxygen stoichiometries of samples were determined by thermogravimetric analysis (TGA) following reduction under a 5% hydrogen/nitrogen gas mixture over the temperature range 20–990°C. Electrical resistivities were measured using the standard four-probe technique. Silver paint was used to attach the four wires to the rectangular pellets.

Results

PXD and TGA Results

The solid solution $Ba_2M_{2-x}Cu_xO_{4+\delta}$ (M = In, Sc) was successfully characterized by powder X-ray diffraction. All indium and scandium compounds were found to be essentially single phase with small impurity peaks at $2\theta \sim 29°$ for higher x values. PXD patterns showed that beyond $x \sim 1$ compounds become multiphase. For $x > 0$ the patterns were indexed using the tetragonal $P4/mmm$ structure as a basis with initial cell parameters of $a \approx 4.1$ Å and $c \approx 8.0$ Å. The $x = 0$ compound however could not be indexed satisfactorily in $P4/mmm$; many additional peaks were observed indicating a lower symmetry. $Ba_2In_2O_5$ was indexed as a Brownmillerite phase crystallizing in space group $Ibm2$.

The cell parameters for unannealed and oxygen annealed samples obtained from the least square refinement are shown in Tables I and II. Oxygen stoichiometries obtained by TGA (typical errors ±0.05) and derived copper valencies are also shown. Electrical resistivity results showed that all these materials were insulating at room temperature.

Results show that at $x = 0$, $Ba_2In_2O_5$, the Brownmillerite structure is adopted. Mader and Müller-Buschbaum found that at 1400°C the composition BaO : In_2O_3 2 : 1 gave a defect perovskite $BaInO_{2.5}$ (*7*). Such a structure was not observed at temperatures of up to 1300°C and presumably a phase transition occurs above 1300°C. $Ba_2In_2O_5$ crystallizes in a larger unit cell than $Sr_2In_2O_5$, reflecting the larger size of Ba^{2+} (r = 1.42 Å) over Sr^{2+} (r 1.25 Å) (*21*).

As copper is substituted for indium, the structure changes to the doubled perovskite observed by Kharlanov *et al.* (*20*). PXD also showed that for $0 < x < 0.5$ sintering at higher temperatures ($T >$ 1050°C) resulted in the tetragonal phases decomposing to a Brownmillerite phase and an unidentified phase. Preliminary attempts to index the $x > 0$ Brownmillerite phases indicate smaller cell parameters than those of $Ba_2In_2O_5$, suggesting possible copper substitution.

For tetragonal $x > 0$ samples lattice parameters and oxygen levels decrease with increasing copper content. The TGA results show that these samples contain *univalent* copper. The reduction in cell size and oxygen content corresponds to replacement of In^{3+} by smaller less positive Cu^+. The loss of oxygen as Cu^+ is substituted suggests the coordination of the metal site(s) onto which Cu^+ is substituting is being reduced from octahedral to square planar and/or linear. The $x = 1$ copper substituted barium scandate also contains Cu^+ implying a metal–oxygen coordination similar to the indium compounds.

Samples show changes in lattice parameters and oxygen levels after oxygen annealing. All three of the annealed samples contain mixed valence copper, Cu^+/Cu^{2+} giving

TABLE I

CELL PARAMETERS AND OXYGEN STOICHIOMETRIES OF UNANNEALED SAMPLES $Ba_2M_{2-x}Cu_xO_y$, M = In, Sc

Sample	Cell parameter			O content	Cu
	a (Å)	b (Å)	c (Å)	y	valence
$Ba_2In_2O_y$	6.0983(7)	16.721(2)	5.9620(9)	5	—
$Ba_2In_{1.7}Cu_{0.3}O_y$	4.2265(14)	4.2265(14)	8.276(3)	4.70	1.00
$Ba_2In_{1.5}Cu_{0.5}O_y$	4.2171(6)	4.2171(6)	8.231(1)	4.51	1.04
$Ba_2In_{1.3}Cu_{0.7}O_y$	4.2077(16)	4.2077(16)	8.202(3)	4.32	1.06
Ba_2InCuO_y	4.1815(12)	4.1815(12)	8.100(2)	4.02	1.04
Ba_2ScCuO_y	4.1270(6)	4.1270(6)	7.966(1)	4.00	1.00

an average copper valence of ~1.4. Lattice parameters do not increase uniformly on annealing. For x = 0.5, M = In, a decreases and c increases. For x = 1, M = In, a increases and c decreases, and for x = 1, M = Sc, both a and c increase. These changes would indicate not only addition but also a marked redistribution of oxygen. Such changes in O-site occupation could lead to increased copper coordination.

Kharlanov *et al.* found that in $Ba_2ScCuO_{4.5}$ the O_I and O_{II} sites were fully occupied and that O_{III} was 25% occupied (*20*). This would imply that in Ba_2MCuO_4 O_{III} is vacant and that as oxygen is added to the system, either by annealing or by substituting M for copper, the O_{III} site becomes partially occupied. A fully occupied O_{III} site, assuming O_I and O_{II} remain fully occupied, would correspond to an oxygen stoichiometry of O_6, i.e., δ = 2. For M = In at x = 0, however, the two $BaInO_{2.5}$ cubes become equivalent and the compound either forms the perovskite or undergoes a phase change to the Brownmillerite structure and hence δ = 2 could never be reached. For a copper-doped sample, the theoretical oxygen limit would suggest impractically high copper oxidation states (e.g., Cu^{5+} in Ba_2MCuO_6).

TABLE II

CELL PARAMETERS AND OXYGEN STOICHIOMETRIES OF OXYGEN-ANNEALED SAMPLES $Ba_2M_{2-x}Cu_xO_y$, M = In, Sc

Sample	Cell parameter		O content	Cu
	a (Å)	c (Å)	y	valence
$Ba_2In_{1.5}Cu_{0.5}O_y$	4.2127(6)	8.253(1)	4.60	1.40
Ba_2InCuO_y	4.1870(6)	8.085(2)	4.19	1.38
Ba_2ScCuO_y	4.1288(7)	7.968(1)	4.17	1.34

Structure Refinement of $Ba_2In_2O_5$

A full profile refinement (*22*) was carried out on $Ba_2In_2O_5$ in the space group *Ibm*2 with $Sr_2In_2O_5$ (*17*) as a basis (interchanging the reported x and z coordinates to comply with the normal crystal structure description of Brownmillerite (*23*)) and using cell parameters calculated from previous PXD runs. Initial cycles included scale factor, zeropoint, background parameters, half-width parameters, and lattice parameters as variables. In final cycles atomic positions, isotropic temperature factors and the asymmetry parameter were allowed to vary. As refinement of profile X-ray data is rather insensitive to temperature factors, due to problems in estimating the background, the isotropic temperature factors of the oxygen sites were refined collectively. The final profile and atomic parameters for the sample are shown in Table III. Tables IV and V record the metal–oxygen bond distances and angles for $Ba_2In_2O_5$. Figure 2 shows the observed, calculated, and difference plots for $Ba_2In_2O_5$. The structure of $Ba_2In_2O_5$ is illustrated in Fig. 3.

TABLE III

FINAL PROFILE AND ATOMIC PARAMETERS FOR $Ba_2In_2O_5$

$Ba_2In_2O_5$

Space group: *Ibm*2 $a = 6.0956(1)$ Å, $b = 16.7112(3)$ Å, $c = 5.9601(1)$ Å

Atom	Wyckoff symbol	x	y	z	B	N
Ba	8*c*	0.0146(4)	0.1094(1)	0.5023(25)	1.58(7)	1.0
In_I	4*a*	0.0000	0.0000	0.0000	1.56(9)	1.0
In_{II}	4*b*	0.9357(7)	0.2500	0.0147(26)	2.82(14)	1.0
O_I	8*c*	0.3121(36)	0.9904(14)	0.2509(54)	0.56(48)	1.0
O_{II}	8*c*	0.0404(30)	0.1423(9)	0.0320(85)	0.56(48)	1.0
O_{III}	4*b*	0.8760(55)	0.2500	0.6245(71)	0.56(48)	1.0

Note. $R_I = 4.08$, $R_{wp} = 13.90$, and $R_e = 3.59$.

The structure of $Ba_2In_2O_5$ resembles $Sr_2In_2O_5$ (*17*) in that it is composed of sheets of corner sharing $In–O_6$ octahedra perpendicular to *b* connected to chains of $In–O_4$ tetrahedra parallel to *c*. Atomic positions are shifted with respect to $Sr_2In_2O_5$, however, and this is perhaps most significant for the three oxygen sites. In $Ba_2In_2O_5$ the corners of the tetrahedra, O_{II}, lie alternately in front of and behind Ba^{2+} in the *ab*-plane, parallel to *c*. The distortion of the In–O polyhedra is marked. This is notable when compared to Brownmillerite (Ca_2FeAlO_5) itself (*23*). For example, the $O_{II}–(Al,Fe)–O_{II}$ bond angle in the $(Al,Fe)O_4$ tetrahedron is 121.3° in Ca_2FeAlO_5; the equivalent $O_{II}–In2–O_{II}$ tetrahedral bond angle in $Ba_2In_2O_5$ is 140.5(25)°. The mean octahedral O–metal–O bond angle in $Ba_2In_2O_5$ is 90.3°(18), as compared to 90.2° in $Ca_2FeAl)_5$, and the mean tetrahedral O–metal–O bond angle in $Ba_2In_2O_5$ is

TABLE IV

BOND LENGTHS IN $Ba_2In_2O_5$

Bond	Number	Distance (Å)
Ba–O1	1	3.080(26)
Ba–O1	1	2.999(1)
Ba–O1	1	2.696(1)
Ba–O1	1	2.550(30)
Ba–O2	1	2.861(61)
Ba–O2	1	3.208(68)
Ba–O2	1	3.432(21)
Ba–O2	1	2.773(9)
Ba–O3	1	2.601(5)
In1–O1	2	2.425(35)
In1–O1	2	1.882(41)
In1–O2	2	2.398(20)
In2–O2	2	1.912(5)
In2–O3	1	2.354(63)
In2–O3	1	2.010(46)

TABLE V

BOND ANGLES IN $Ba_2In_2O_5$

Atoms	Number	Angle (°)
Indium–oxygen octahedron		
O1–In1–O1	1	103.9(1)
O1–In1–O1	1	75.8(1)
O1–In1–O1	2	90.2(3)
O1–In1–O2	2	92.3(16)
O1–In1–O2	2	94.9(1)
O1–In1–O2	2	88.0(1)
O1–In1–O2	2	86.3(25)
Indium–oxygen tetrahedron		
O2–In2–O2	1	140.5(25)
O2–In2–O3	2	107.3(2)
O2–In2–O3	2	96.0(19)
O3–In2–O3	1	100.1(20)

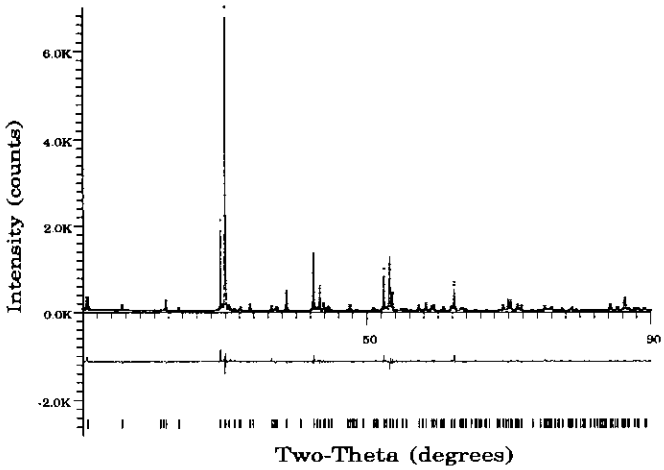

FIG. 2. Observed, calculated, and difference plots of $Ba_1In_2O_5$.

107.94°(14), as compared to 109.4° in Ca_2FeAlO_5.

The unit cell of $Ba_2In_2O_5$ is, as expected, larger than that observed for $Sr_2In_2O_5$ (*17*). The lattice parameters calculated from the refinement are in reasonable agreement from those calculated from earlier runs. The increase in lattice parameters is most significant in the *b* direction where complete replacement of Sr^{2+} by Ba^{2+} results in an expansion in *b* of ~6%. The expansion of the unit cell is controlled by the Ba–O bond distances. In $Ba_2In_2O_5$, the mean Ba–O bond distance is 2.911(24) Å. The equivalent Sr–O mean bond distance in $Sr_2In_2O_5$ is 2.698 Å.

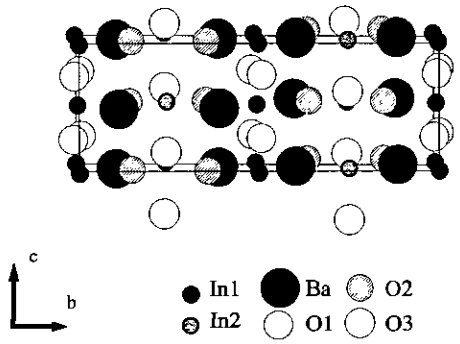

FIG. 3. The structure of $Ba_2In_2O_5$.

The coordination of the alkaline earth metal ion in Brownmillerite structures increases with ion size. In Ca_2FeAlO_5, Ca^{2+} is surrounded by seven oxygens at a mean distance of 2.461 Å (*23*). In $Sr_2In_2O_5$ (*17*) and $Sr_2Fe_2O_5$ (*24*), Sr^{2+} lies in eightfold coordination with oxygen at mean distances of 2.698 and 2.628 Å, respectively. In $Ba_2In_2O_5$, Ba^{2+} is nine-coordinate with a mean Ba–O distance of 2.911(24) Å. The Ba–O bond distances vary from 2.550(30) to 3.432(21) Å in $Ba_2In_2O_5$ and such distances are not uncommon in barium in dates (for example, Ba–O distances of 3.340(14) Å in $BaSr_2In_6O_{12}$ (*14*) and 3.338(1) Å in Ba_2InAlO_5 (*25*)).

The In2–O tetrahedron mean bond distances are similar in both the barium (2.047(29) Å) and strontium (2.035 Å compounds. The In1–O octahedron is larger in $Ba_2In_2O_5$ than in $Sr_2In_2O_5$, however, with a mean In1–O bond length of 2.235(22) Å as compared to 2.163 Å in $Sr_2In_2O_5$. In Ca_2FeAlO_5 the metal tetrahedra and octahedra are reported to elongate along the *b*-axis (*23*). This distortion also occurs in $Sr_2In_2O_5$ (*17*) and $Sr_2Fe_2O_5$ (*24*). An analogous elongation of In–O polyhedra along *b* is not exhibited in $Ba_2In_2O_5$. The In1–O octahedron is composed of two sets of two longer In–O

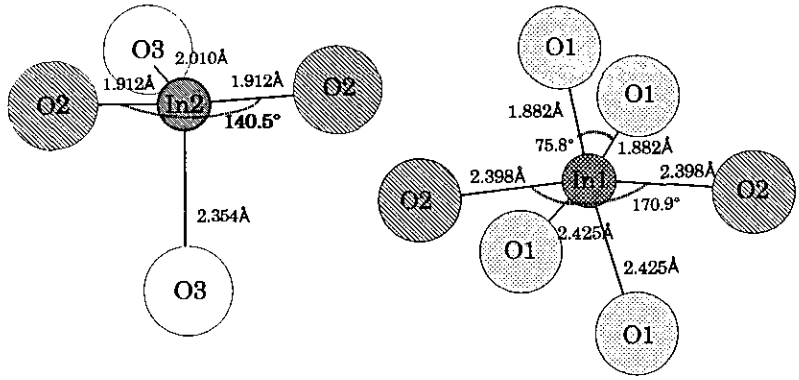

FIG. 4. Coordination polyhedra of In^{3+} in $Ba_2In_2O_5$

bonds, one set parallel (2.425(35) Å) to and one set perpendicular (2.398(20) Å) to *b*. The remaining two bonds are much shorter (1.882(41) Å) and run perpendicular to *b*. The In–O tetrahedra are elongated perpendicular to *b* with shorter In–O_{II} bonds (1.912(5) Å) parallel to *b*. The indium–oxygen coordination polyhedra are shown in detail in Fig. 4.

Structure Refinements of "Doubled Perovskite" Phases

Full profile refinements (*22*) were carried out on the unannealed samples M= In, x = 0, 0.5, 1 and M = Sc, x = 1. Refinements were also performed on oxygen annealed M = In, x = 0.5, 1 and M = Sc, x = 1. The refinements were carried out in space group *P4/mmm* based on $Ba_2ScCuO_{4.5}$ (*20*) using lattice parameters obtained from earlier PXD runs. PXD intensity data for the 001 reflection in the M= In compounds showed a relatively intense peak suggesting a B cation distribution with In on the B1 (0,0,0) site. Sc had been observed to occupy the (0,0,0) site in $Ba_2ScCuO_{4.5}$ (*20*). Initially, therefore, M and Cu ions were ordered on the two available B sites, with M on the B1 site (0,0,0). Early refinements allowed scale factor, zeropoint, background coefficients, halfwidth parameters and cell parameters to vary. Final cycles included atomic positions, isotropic temperature factors and occupancies of metal and oxygen sites.

For unannealed and annealed samples of $Ba_2In_{1.5}Cu_{0.5}O_{4+\delta}$ and unannealed Ba_2InCuO_4 variation of M (In) occupancy indicated a strong preference for the *B*1 (0,0,0) site as anticipated (negative occupancies were observed for Cu on the *B*1 site) and this, therefore, was fixed at unity in final refinement cycles. In each case oxygen and metal isotropic temperature factors could not be refined simultaneously without instability in the refinement; therefore cation and anion isotropic temperature factors were not always refined simultaneously. Tables VI–XI show the final profile and atomic parameters of the materials. Figures 5 and 6 show the observed, calculated and difference plots for the refinements of the oxygen annealed M = In, x = 0.5 sample, $Ba_2In_{1.5}Cu_{0.5}O_{4.6}$, and the unannealed M = Sc, x = 1 sample, Ba_2ScCuO_4. Bond lengths of the indium and scandium compounds are shown in Tables XII and XIII.

M = In, x = 0.5 Samples

The M= In, x = 0.5 samples have a cation distribution in which In^{3+} wholly occupies the *B*1 (0,0,0) site and shares the *B*2 (0,0,0.5) site with Cu^{n+} (where $n > 1$ in oxygen-annealed samples). In unannealed samples the apical oxygen of the In/Cu octahedron, O_{II} (0,0,z), is displaced from its "ideal" position of z = 0.25 toward the shared In/Cu *B*2 site and hence the *B*2–O_{II} bond (1.908(23) Å) is significantly shorter than the

TABLE VI

FINAL PROFILE AND ATOMIC PARAMETERS FOR $Ba_2In_{1.5}Cu_{0.5}O_{4.5}$

$BaIn_{1.5}Cu_{0.5}O_4$ unannealed

Space group: $P4/mmm$ a = 4.2152(1) Å, c = 8.2264(2) Å

Atom	Wyckoff symbol	x	y	z	B	N
Ba	2*h*	0.5	0.5	0.2279(2)	0.42(5)	1.0
B1	1*a*	0	0	0	0.44(10)	1.0 In
B2	1*b*	0	0	0.5	2.76(18)	0.5 In 0.5 Cu
O_I	2*f*	0.5	0	0	2.79(62)	1.0
O_{II}	2*g*	0	0	0.2681(28)	2.30(67)	0.95(2)
O_{III}	2*e*	0.5	0	0.5	3.00	0.31(2)

Note. R_I = 4.71, R_{wp} = 13.58, and R_e = 3.44.

$B1$–O_I bond (2.206(23) Å). This observation concurs with a smaller $B2$ site consisting of In^{3+} and Cu^+, considering Cu^+ typically forms oxygen bonds of ~1.8 Å. The O_I site is fully occupied and the O_{II} site is almost wholly occupied in the unannealed sample. The O_{III} site is approximately one third occupied.

The distribution of oxygen creates a mean ninefold coordination for Ba^{2+} as observed in $Ba_2ScCuO_{4.5}$ (*20*). The Ba site is displaced from its "ideal" position (0.5,0.5,0.25) toward the layer of fully occupied O_I sites. The In^{3+} ($B1$) coordination is almost octahedral with the 95% occupied axial O_{II} sites leading to a mean coordination just below 6. The In "octahedron" is distorted with two longer axial bonds parallel to c. The $B2$ Cu/In coordination is more complex. The much shorter $B2$–O_{II} bonds are reminiscent of the dumbbell coordination of Cu reported in $Ba_2ScCuO_{4.5}$ (*20*). The net coordination of the $B2$ site is a distorted partially filled octahedron elongated in the plane perpendicualr to c.

In the oxygen annealed material the distribution and position of anions change markedly. The O_I site remains 100% occupied but the occupancy of O_{II} drops from almost

TABLE VII

FINAL PROFILE AND ATOMIC PARAMETERS FOR $Ba_2In_{1.5}Cu_{0.5}O_{4+\delta}$

$BaIn_{1.5}Cu_{0.5}O_{4+\delta}$ Oxygen annealed

Space group: $P4/mmm$ a = 4.2120(1) Å, c = 8.2528(3) Å

Atom	Wyckoff symbol	x	y	z	B	N
Ba	2*h*	0.5	0.5	0.2257(3)	0.93(9)	1.0
B1	1*a*	0	0	0	0.08(12)	1.0 In
B2	1*b*	0	0	0.5	1.89(19)	0.5 In 0.5 Cu
O_I	2*f*	0.5	0	0	0.50	1.0
O_{II}	2*g*	0	0	0.2507(38)	0.50	0.66(2)
O_{III}	2*e*	0.5	0	0.5	0.50	0.64(2)

Note. R_I = 8.05, R_{wp} = 14.88, and R_e = 3.39.

TABLE VIII

FINAL PROFILE AND ATOMIC PARAMETERS FOR $Ba_2In_{1.5}Cu_{0.5}O_{4.5}$

$BaInCuO_4$ unannealed

Space group: *P4/mmm* a = 4.1827(1) Å, c = 8.0982(2) Å

Atom	Wyckoff symbol	x	y	z	B	N
Ba	2*h*	0.5	0.5	0.2335(3)	0.01	1.0
B1	1*a*	0	0	0	0.01	1.0 In
B2	1*b*	0	0	0.5	1.86(26)	1.0
O_I	2*f*	0.5	0	0	0.32(52)	1.0
O_{II}	2*g*	0	0	0.2880(29)	0.04(79)	0.75(2)
O_{III}	2*e*	0.5	0	0.5	0.3	0.25(2)

Note. R_I = 4.63, R_{wp} = 13.37, and R_e = 3.00.

100 to 66%. The remainder moves on to the O_{III} site and additional oxygen preferentially occupies O_{III}. The O_{II} oxygen shifts back towards the *B*1 site close to its "ideal" position and hence *B*1–O_{III} and *B*2–O_{II} are equidistant within experimental error. The increased oxygen level determined by TGA and confirmed by the structure refinement implies a copper valence of 1.4, i.e., a mixture of Cu^+ and Cu^{2+}. The increased size of the mixed *B*2 site of $In^{3+}/Cu^+/Cu^{2+}$ (50%/30%/20% approx.) increases the length of the *B*2–O_{II} bond. This is consistent with replacement of Cu^+ by Cu^{2+}, the latter having a similar ionic radius to In^{3+} in six-fold coordination ($r_{In^{3+}}$ = 0.79 Å, $r_{Cu^{2+}}$ = 0.73 Å) (*21*).

Kharlanov *et al.* report broad ranges of solid solutions $Ba_2M_{1\pm x}Cu_{1\pm x}O_{4.5\pm x/2}$ (M = In, Sc, Lu) in which changes of the ratio M/Cu produce changes in the a parameter but no noticeable change in c (*20*). They suggest this would imply a statistical distribution of M and Cu across the solid solution, leading to equally sized *B*1 and *B*2 sites and hence equal length *B*1–O_{II} and *B*2–O_{II} bonds. This suggestion, however, is not consistent with their PXD structure refinement of $Ba_2ScCuO_{4.5}$ nor with the results above. The cat-

TABLE IX

FINAL PROFILE AND ATOMIC PARAMETERS FOR $Ba_2InCuO_{4+\delta}$

$BaInCuO_{4+\delta}$ oxygen annealed

Space group: *P4/mmm* a = 4.1867(1) Å, c = 8.0894(2) Å

Atom	Wyckoff symbol	x	y	z	B	N
Ba	2*h*	0.5	0.5	0.2374(4)	0.42(7)	1.0
B1	1*a*	0	0	0	0.01	0.95(1) In 0.05(1) Cu
B2	1*b*	0	0	0.5	3.63(55)	0.95(1) Cu 0.05(1) In
O_I	2*f*	0.5	0	0	0.01	1.0
O_{II}	2*g*	0	0	0.2815(43)	0.01	0.74(2)
O_{III}	2*e*	0.5	0	0.5	0.49(89)	0.36(2)

Note. R_I = 5.73, R_{wp} = 14.83, and R_e = 3.20.

TABLE X

FINAL PROFILE AND ATOMIC PARAMETERS FOR Ba_2ScCuO_4

$BaScCuO_4$ unannealed

Space group: $P4/mmm$ a = 4.1240(1) Å, c = 7.9666(2) Å

Atom	Wyckoff symbol	x	y	z	B	N
Ba	2*h*	0.5	0.5	0.2356(2)	0.30(5)	1.0
B1	1*a*	0	0	0	0.29(24)	0.98(2) Sc 0.02(2) Cu
B2	1*b*	0	0	0.5	2.29(25)	0.98(2) Cu 0.02(2) Sc
O_I	2*f*	0.5	0	0	0.23(41)	1.0
O_{II}	2*g*	0	0	0.2822(24)	0.01	0.82(1)
O_{III}	2*e*	0.5	0	0.5	0.01	0.18(1)

Note. R_I = 3.27, R_{wp} = 11.68, and R_e = 2.76.

ion distribution of $Ba_2In_{1.5}Cu_{0.5}O_{4.5}$ indicates that Cu is substituted for In preferentially on the *B*2 site. This postulate is confirmed both by the reluctance of Cu to occupy the *B*1 in the refinements and by the limit of the solid solution at x = 1 (beyond which Cu would be forced to partially occupy the *B*1 site). Furthermore, PXD results describe a solid solution in which both a and c decrease linearly with copper content, x. The percentage decrease in c across the solid solution is twice that of a. This would also imply distinct In and In/Cu sites with an a parameter controlled by the In–O_I bond length. Copper, therefore, substitutes preferentially on to the *B*2 (0, 0, 0.5) site across the solid solution until at x = 1 the *B*2 site is solely occupied by Cu.

M = In, x = Samples

Unannealed Ba_2InCuO_4 does not have a cation distribution as described by Kharlanov *et al.* where In and Cu are statistically distributed across the B sites (*20*), but is

TABLE XI

FINAL PROFILE AND ATOMIC PARAMETERS FOR $Ba_2ScCuO_{4+\delta}$

$BaScCuO_{4+\delta}$ oxygen annealed

Space group: $P4/mmm$ a = 4.1247(1) Å, c = 7.9632(2) Å

Atom	Wyckoff symbol	x	y	z	B	N
Ba	2*h*	0.5	0.5	0.2366(3)	0.58(7)	1.0
B1	1*a*	0	0	0	0.97(34)	0.87(3) Sc 0.13(3) Cu
B2	1*b*	0	0	0.5	2.12(32)	0.87(3) Cu 0.13(3) Sc
O_I	2*f*	0.5	0	0	0.41(53)	1.0
O_{II}	2*g*	0	0	0.2786(30)	0.01	0.84(1)
O_{III}	2*e*	0.5	0	0.5	0.01	0.26(1)

Note. R_I = 3.83, R_{wp} = 14.14, and R_e = 2.80.

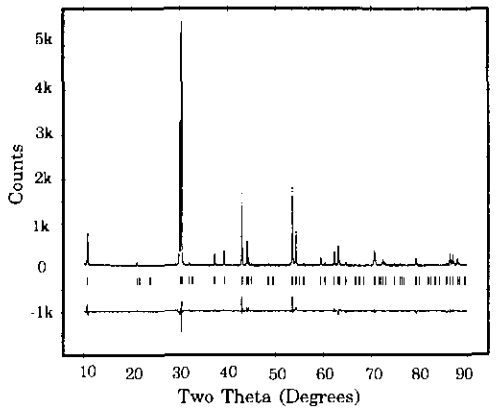

FIG. 5. Observed, calculated, and difference plots of $Ba_2In_{1.5}Cu_{0.5}O_{4.6}$.

similar to $Ba_2ScCuO_{4.5}$, with Cu fully occupying the $B2$ (0, 0, 0.5) site and In ordered on the $B1$ site (0, 0, 0). The structure refinement confirms TGA data of an oxygen level of 4 (i.e., $\delta = 0$) and Cu is substituted as Cu^+. Like $Ba_2In_{1.5}Cu_{0.5}O_{4.5}$, the O_I site is fully occupied, the occupancy of O_{II}, however, is reduced to 75% with the remainder of the oxygen on O_{III} (25% occupied).

The significant difference in sizes of the two B sites leads to very different B–O_{II} bond lengths. The axial oxygen, O_{II}, shifts dramatically away from the ideal position (0, 0, 0.25) toward the Cu ($B2$) site. The resulting $B2$–O_{II} distance is small (1.717(23) Å) and characteristic of a Cu^+–O bond. The coordination environment of the copper site is one of a significantly distorted octhedron with two very short axial bonds and four (1.5 on average) much longer equatorial bonds in the *ab*-plane. The shape of the indium octahedron is the inverse of this with elongation of the axial (In–O_{II}) bonds along *c*. Barium is surrounded by 12 oxygens as in $BaInO_{2.5}$ (*7*) but is lowered to a mean coordination of 8 due to the partially occupied O_{II} and O_{III} sites. As in $Ba_2In_{1.5}Cu_{0.5}O_{4.5}$, Ba^{2+} is displaced toward the InO_I layer and hence the Ba coordination polyhedron is made up of four shorter Ba–O_I bonds and two sets of four longer almost equidistant bonds to O_{II} and O_{III}.

After oxygen annealing the oxygen level rises by $\delta = 0.2$. The O_I site remains fully occupied and the occupancy of O_{II} is essentially unchanged at ≈75%. Additional oxy-

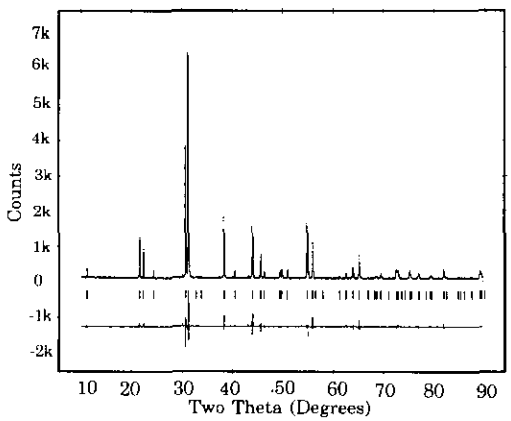

FIG. 6. Observed, calculated, and difference plots of Ba_2ScCuO_4.

TABLE XII

BOND LENGTHS IN UNANNEALED $Ba_2M_{2-x}Cu_xO_{4+\delta}$ COMPOUNDS

Bond	Number	Distance (Å)		
		$Ba_2In_{1.5}Cu_{0.5}O_{4.5}$	Ba_2InCuO_4	$BaScCuO_4$
Ba–O1	4	2.821(1)	2.830(1)	2.788(1)
Ba–O2	4	2.999(2)	2.988(3)	2.940(2)
Ba–O3	4	3.074(1)	2.993(1)	2.948(1)
B1–O1	4	2.108(1)	2.091(1)	2.062(1)
B1–O2	2	2.206(23)	2.332(23)	2.248(19)
B2–O2	2	1.908(23)	1.717(23)	1.735(19)
B2–O3	4	2.108(1)	2.091(1)	2.062(1)

TABLE XIII

BOND LENGTHS IN OXYGEN-ANNEALED $Ba_2M_{2-x}Cu_xO_{4+\delta}$ COMPOUNDS

Bond	Number	Distance (Å)		
		$Ba_2In_{1.5}Cu_{0.5}O_{4.6}$	$Ba_2InCuO_{4.2}$	$BaScCuO_{4.2}$
Ba–O1	4	2.812(1)	2.841(2)	2.793(1)
Ba–O2	4	2.985(2)	2.982(4)	2.936(2)
Ba–O3	4	3.092(1)	2.982(2)	2.942(1)
B1–O1	4	2.106(1)	2.093(1)	2.062(1)
B1–O2	2	2.069(32)	2.277(35)	2.219(24)
B2–O2	2	2.057(32)	1.768(35)	1.763(24)
B2–O3	4	2.106(1)	2.093(1)	2.062(1)

gen preferentially substitutes on to the O_{III} site to a level of 36%. Another possible consequence of oxygen annealing is the redistribution of cations between the $B1$ and $B2$ sites. The very small amount of Cu refined on the $B1$ site (95% In, 5% Cu), however, is probably not significant and the ordered distribution reported by Kharlanov *et al.* in the equivalent scandate (where the oxygen level had been raised to $\delta = 0.5$) (*20*) is probably more likely.

As in $Ba_2In_{1.5}Cu_{0.5}O_{4.6}$, increased oxygen levels and hence partial substitution of Cu^{2+} for Cu^+ results in shifts in Ba and O_{II} positions and, therefore, leads to changes in Ba–O, $B1$–O, and $B2$–O bond lengths. Unlike $Ba_2In_{1.5}Cu_{0.5}O_{4.6}$, however, Ba shifts away from the $B1$–O_I layer towards the $B2$–O_{III} layer. The coordination of the Ba site does not change appreciably with slight elongation of the Ba–O_I bonds and conversely slight reduction of Ba–O_{II} and Ba–O_{III} bond lengths. The Ba–O_{II} and Ba–O_{III} distances remain equal. The shift of O_{II} toward the $B1$ site increases the $B2$–O_{II} bond length as in $Ba_2In_{1.5}Cu_{0.5}$ $O_{4.6}$. The $B2$–O_{II} bond remains small (1.768(35) Å) despite 40% substitution of Cu^{2+} for Cu^+. This is perhaps not unusual, however, considering a Cu^{2+}–O_{II} bond length of 1.81(9) Å was reported in $Ba_2ScCuO_{4.5}$ (*20*). The shape of the coordination polyhedra of the $B1$ and $B2$ cations remain essentially unchanged despite an increased mean coordination for $B2$; the $B1$ octahedron elongated along c, the $B2$ octahedron elongated in the *ab*-plane.

Following oxygen annealing, $Ba_2InCuO_{4+\delta}$ increases in a and decreases in c. The opposite is observed for $Ba_2In_{1.5}Cu_{0.5}O_{4+\delta}$. In each case it is the change in the c-parameter that is significant. In the $x = 0.5$ samples after annealing the expansion of the $B2$–O_{II} bond is greater than the contraction of the $B1$–O_{II} bond leading to an increase in c. The converse is true for the $x = 1$ samples.

M = Sc, x = 1 Samples

Unannealed Ba_2ScCuO_4 has an essentially ordered arrangement of cations as reported by Kharlanov *et al.* for $Ba_2ScCuO_{4.5}$ (*20*) and is isostructural to Ba_2InCuO_4 with Cu fully occupying the $B2$ site. The oxygen level of the unannealed sample is 4 as determined by TGA and as in the indium materials the O_I site is fully occupied. The refined oxygen distribution across the O_{II} and O_{III} site is also similar. In the scandium compound the O_I site is 82% occupied (as compared to 75% in Ba_2InCuO_4) and the O_{III} site is 18% occupied (as compared to 25% in Ba_2InCuO_4).

As in the indium materials, the $B1$–O_{II} and $B2$–O_{II} bonds are very different in length. Replacing In^{3+} by smaller Sc^{3+}, however, reduces the size of the $B1$ site and decreases the length of the $B1$–O_I bond. The position of the O_{II} axial oxygen site is effectively unchanged by the complete replacement of In^{3+} by Sc^{3+}. The $B2$ (Cu)–O_{II} bond length (1.735(19) Å) is, therefore, not affected significantly by the $B1$ cation in these compounds. The cell parameters of $Ba_2InCuO_{4.5}$, $Ba_2ScCuO_{4.5}$, and $Ba_2LuCuO_{4.5}$ (*20*), considering the ionic radii of oxygen and the cations concerned (*21*), indicate a constant Cu–O_{II} bond length with a changing $B1$ cation size.

The coordination polyhedra of the $B1$ and $B2$ sites in Ba_2ScCuO_4 are very similar to those of the equivalent indium material. The $B2$ copper octahedron is distorted with four longer equatorial bonds in the *ab*-plane and two much shorter bonds parallel to c. The $B1$ scandium octahedron is less distorted than the indium equivalent but retains the feature of two longer axial Sc–O_{II} bonds along c. As in the indates, Ba^{2+} moves toward the $B1$–O_I layer creating a distorted 12-coordinate polyhedron (of mean coordination 8) with four shorter Ba–O_I bonds and two groups of four longer bonds to O_{II} and O_{III}.

The process of oxygen annealing has much the same effect on the scandate as on the analogous indate compound. The oxygen level rises by $\delta \sim 0.2$, O_I remains fully occupied and the occupation of the O_{II} site remains constant (at $\approx$82%). All the addi-

tional oxygen is located on the O_{III} site as in $Ba_2InCuO_{4.2}$. Again, the distribution of oxygen across the O_{II} and O_{III} sites is similar in the scandate (O_{II} : O_{III} 84% : 26% compared to 74%–36% in $Ba_2InCuO_{4.2}$). A possible redistribution of M and Cu among the *B* sites following annealing is observed. As in Ba_2InCuO_4 this disordering is unlikely. Although the refinement showed the *B*2 site to be 13% occupied by Sc^{3+}, the similarities in scattering factors of Cu and Sc make such an observation unreliable. Kharlanov *et al.* reported an ordered arrangement of *B* cations in $Ba_2ScCuO_{4.5}$ (*20*).

The increase of oxygen on the O_{III} site causes a shift in the Ba position toward the *B*2–O_{III} layer. Although the Ba–O_I bonds lengthen by a small amount, the distortion of the barium–oxygen polyhedra is unchanged with the Ba–O_{II} and Ba–O_{III} distances equal. The O_{II} site is displaced toward *B*1 and the *B*2–O_{II} bond length increases. The *B*2–O_{III} bond distance is much the same as that observed in $Ba_2InCuO_{4.2}$. The characteristic distortion of the *B*1 and *B*2 octahedra is effectively unaltered.

The cell parameters of the scandate changes after oxygen annealing in a similar fashion to the indate with an increase in *a* and a more significant decrease in *c*. The bond length results suggest that in these $x = 1$ materials, the contraction of the *B*1–O_{II} bond is more significant than the expansion of the *B*2–O_{II} bond. However, the errors in these distances are too large to be certain of what is quite a subtle change. The small, almost negligible, changes in the *a*-parameter can be rationalized in terms of what is an essentially fixed distance controlled by the *B*1–O_I bond length. For an essentially ordered arrangement of *B* cations, the *a*-parameter would not be expected to vary with the occupancy of the O_{III} site unless M^{3+} were smaller than Cu^{n+} (where $n \geq 1$). The decrease in *c* is more difficult to rationalise. The substitution of larger Cu^{2+} for Cu^{+} would be expected to prompt an increase in the *c*-parameter. An essentially six-coordinate Cu^{2+} would be expected to have longer axial bonds through Jahn–Teller distortion. That this expansion in *c* is not observed perhaps suggests two things: first, that due to the partial vacancy of the O_{II} and O_{III} sites, Cu^{2+} does not behave as an octahedrally coordinated ion leading to shorter Cu(II)–O bonds, and second, that because an, albeit small, change does occur in *a*, mixing of cations across the *B* sites certainly does occur in oxygen annealed samples. If Cu^{2+} were to preferentially substitute on to the *B*2 site, for example, and an amount of Cu^{+} and M^{3+} were to swap sites, then some contraction of the *B*1–O_{II} bond would be expected.

Discussion

The series of compounds $Ba_2M_{2-x}Cu_xO_{4+\delta}$ (M = In, Sc, Lu) bear many structural similarities to high temperature superconducting cuprates. Raveau *et al.* classified these superconducting materials under the general formula $[ACuO_{3-x}]_m^P$ $[AO]_n^{RS}$ where P = perovskite, RS = rock salt, and *m* and *n* are the integral number of layers of perovskite and rock salt respectively (*26*). The $Ba_2M_{2-x}Cu_xO_{4+\delta}$ materials are really a special case under this general description as they contain no rock-salt-type layers (or one shared layer) and would be classified as $m = \infty$, $n = 0$ structures similar to $YBa_2Cu_3O_{7-\delta}$ and $Ca_{1-x}Sr_xCuO_2$. Furthermore, they are unlike the superconducting cuprates above in that the perovskite *B* site is not solely occupied by copper. In these doubled perovskite compounds the *B* sites become unequivalent. More generally these "multiple-perovskites" could be classified by the expression: $[AB1_{1\pm y}B2_{1\mp y}O_{3-x}]_{m'}$ (where m' = the number of perovskite layers in the unit cell), or more specifically: $[AM_{1\pm y}Cu_{1\mp y}O_{3-x}]_{m'}$ (where *M* is a trivalent metal; In, Sc, Lu).

The "doubled perovskites," however, possess several important structural features which set them apart from superconducting cuprates. Kharlanov et al pointed out that the equatorial Cu–O distances in

the doubled perovskite materials are longer than the optimum distances found in superconducting cuprates. They also drew attention to the need for copper to fully occupy discrete sites and thus create the $[CuO_2]_\infty$ layers apparently essential to produce superconductivity (*20*). Another essential feature of high T_c superconducting materials is the presence of mixed valence copper, usually Cu^{2+}/Cu^{3+}, resulting from an oxygen nonstoichiometry.

To date, the doubled perovskite phases investigated have not possessed all of these important criteria. The ordering of copper on to the (0, 0, 0, 5) *B*2 site allows the creation of $[CuO_2]_\infty$ layers; this ordering may only occur for fixed valence copper ions. In Ba_2MCuO_4 (M = In, Sc), Cu^+ occupies the *B*2 site in an effectively linear coordination with oxygen and no infinite layer structure exists. In $Ba_2MCuO_{4.5}$ (*20*) (M = In, Sc, Lu), Cu^{2+} occupies the *B*2 site and approaches octahedral coordination with oxygen which would create the desired infinite layer structure. Between these two extremes, however, when copper is present as Cu^+/Cu^{2+}, a *B* site disordering may occur. Whether a disordering might occur for mixed valence Cu^{2+}/Cu^{3+} is uncertain as an oxygen level of $\delta > 0.5$ has not yet been achieved.

In these materials the smallest Cu–O equatorial bond distance is ~2.06 Å as compared to ~1.95 Å in superconducting cuprates. This bond length is clearly controlled by the *M*–O equatorial bond distance and hence by the size of *M*. Decreasing the size of the *M* ion will certainly reduce this Cu–O distance, yet, the length of the Cu–O bond can also be engineered by substitution of *A*. Partial or complete substitution of a smaller alkaline earth for barium would lead to shorter *M*–O bonds. For example, in $Sr_2In_2O_5$ (*17*), In–O bond lengths of 1.97 Å have been reported. Sc^{3+} is a smaller cation of similar size to copper and substitution of the *A* cation could produce Cu–O bond distances very close to the optimum observed in high T_c materials.

Clearly, these materials present plenty of scope for future investigation. High-pressure oxygen annealing will be used to try to increase the oxygen level above $\delta = 0.5$ and powder neutron diffraction studies will shortly be carried out to precisely determine the cation distribution and oxygen site positions and occupations in these materials.

Acknowledgments

We thank SERC for the studentship of DHG, and S.E. Dann for her assistance in the identification and indexing of the structure of $Ba_2In_2O_5$.

References

1. F. R. Cruickshank, D. McK. Taylor, and F. P. Glasser, *J. Inorg. Nucl. Chem.* **26,** 937 (1964).
2. W. Kwestroo, H. C. A. van Gerven, and C. Langereis, *Mater. Res. Bull.* **12,** 157 (1977).
3. L. M. Kovba, L. N. Lykova, and T. A. Kalinina, *Russ. J. Inorg. Chem.* **25,** 397 (1980).
4. T. A. Kalinina, L. N. Lykova, L. M. Kovba, M. G. Mel'nikova, and N. V. Porotnikov, *Russ. J. Inorg. Chem.* **28,** 259 (1983).
5. K. Mader and Hk. Müller-Buschbaum, *Z. Anorg. Allg. Chem.* **559,** 89 (1988).
6. A. Lalla and Hk. Müller-Buschbaum, *Z. Anorg. Allg. Chem.* **573,** 12 (1989).
7. K. Mader and Hk. Müller-Buschbaum, *Z. Anorg. Allg. Chem.* **528,** 125 (1985).
8. F. Kanamaru and M. Koizumi, *J. Am. Ceram. Soc.* **56,** 399 (1973).
9. K. Mader and Hk. Müller-Buschbaum, *J. Less-Common Met.* **157,** 71 (1990).
10. Y. S. Zhen and J. B. Goodenough, *Mater. Res. Bull* **25,** 785 (1990).
11. A. Lalla and Hk. Müller-Buschbaum, *J. Less-Common Met.* **154,** 233 (1989).
12. R. v.Schenck and Hk. Müller-Buschbaum, *Z. Anorg. Allg. Chem.* **398,** 24 (1973).
13. A. Lalla and Hk. Müller-Buschbaum, *Z. Anorg. Allg. Chem.* **588,** 117 (1990).
14. A. Lalla and Hk. Müller-Buschbaum, *Rev. Chim. Miner.* **24,** 1 (1987).
15. R. v.Schenk and Hk. Müller-Buschbaum, *Z. Anorg. Allg. Chem.* **398,** 15 (1973).
16. W. Muschick and Hk. Müller-Buschbaum, *Z. Anorg. Allg. Chem.* **435,** 56 (1977).
17. R. v.Schenck and Hk. Müller-Buschbaum, *Z. Anorg. Allg. Chem.* **395,** 280 (1973).
18. W. Kwestroo, H. A. M. van Hal, and C. Langereis, *Mater. Res. Bull.* **9,** 1623 (1974).
19. L. M. Kovba and M. V. Paramova, *Vestn. Mosk. Univ. Khim.* **11,** 621 (1970).
20. A. L. Kharlanov, N. R. Khasanova, M. V.

PAROMOVA, E. V. ANTIPOV, L. N. LYKOVA, AND L. M. KOVBA, *Russ. J. Inorg. Chem.* **35,** 1741 (1990).
21. R. D. SHANNON AND C. T. PREWITT, *Acta Crystallogr. Sect. B* **25,** 925 (1969).
22. H. M. RIETVELD, *Acta. Crystallogr.* **22,** 151 (1967).
23. A. A. COLVILLE AND S. GELLER, *Acta Crystallogr. Sect. B* **27,** 2311 (1971).
24. M. HARDER AND HK. MÜLLER-BUSCHBAUM, *Z. Anorg, Allg. Chem.* **464,** 169 (1980).
25. HK. MÜLLER-BUSCHBAUM AND M. ABED, *Z. Anorg. Allg. Chem.* **591,** 174 (1990).
26. B. RAVEAU, C. MICHEL, M. HERVIEU, D. GROULT, AND J. PROVOST, *J. Solid State Chem.* **85,** 181 (1990).